Article

Theoretical Studies on the Hydrolysis of Mono-Phosphate and Tri-Phosphate in Gas Phase and Aqueous Solution

Yan-Ni Wang, Igor A. Topol, Jack R. Collins, and Stanley K. Burt

J. Am. Chem. Soc., **2003**, 125 (43), 13265-13273• DOI: 10.1021/ja0279794 • Publication Date (Web): 02 October 2003

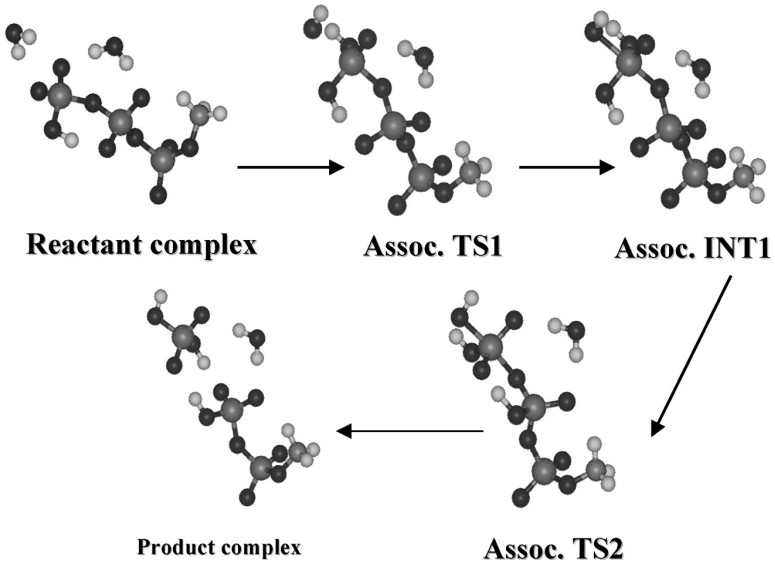

More About This Article

Additional resources and features associated with this article are available within the HTML version:

- Supporting Information
- Links to the 8 articles that cite this article, as of the time of this article download
- Access to high resolution figures
- Links to articles and content related to this article
- Copyright permission to reproduce figures and/or text from this article

View the Full Text HTML

J|A|C|S
ARTICLES
Published on Web 10/02/2003

Theoretical Studies on the Hydrolysis of Mono-Phosphate and Tri-Phosphate in Gas Phase and Aqueous Solution

Yan-Ni Wang, Igor A. Topol, Jack R. Collins, and Stanley K. Burt*

Contribution from the Advanced Biomedical Computing Center, National Cancer Institute at Frederick, P.O. Box B, Frederick, Maryland, 21702

Received August 1, 2002; Revised Manuscript Received April 25, 2003; E-mail: burt@ncifcrf.gov

Abstract: Phosphate hydrolysis by GTPases plays an important role as a molecular switch in signal transduction and as an initiator of many other biological processes. Despite the centrality of this ubiquitous reaction, the mechanism is still poorly understood. As a first step to understand the mechanisms of this process, the nonenzymatic hydrolysis of mono-phosphate and tri-phosphate esters were systematically studied in gas phase and aqueous solution using hybrid density functional methods. The dielectric effect of the environment on the energetics of these processes was also explored. Theoretical results show that for mono-phosphate ester, the dissociative pathway is much more favorable than the associative pathway. However, the reaction barriers for the dissociative and associative pathways of tri-phosphate hydrolysis are very close in aqueous solution, though the dissociative pathway is more favorable in the gas phase. High dielectric solvents, such as water, significantly lower the activation barrier of the associative pathway due to the greater solvation energy of the associative transition states than that of the reactant complex. By contrast, the barrier of the dissociative pathway, with respect to the gas phase, is less sensitive to the surrounding dielectric. In the associative hydrolysis pathway of the tri-phosphate ester, negative charge is transferred from the γ-phosphate to β-phosphate through the bridging ester oxygen and results in $P_\gamma-O$ bond dissociation. No analogous charge transfer was observed in the dissociative pathway, where $P_\gamma-O$ bond dissociation resulted from proton transfer from the γ-phosphate to the bridge oxygen. Finally, the active participation of local water molecules can significantly lower the activation energy of the dissociative pathway for both mono-phosphate and tri-phosphate.

Introduction

Hydrolysis of phosphate, such as GTP, plays an important role in many biological processes. The enzymatic GTPase molecular switch is a universal mechanism used to regulate biochemical pathways that operates through the ability to undergo a guanine nucleotide-dependent conformational change. Molecular target identification and interaction is controlled by the conformational state of the specific enzyme within the GTPase super-family. The GTPase "active", GTP bound, state remains active until GTP is hydrolyzed to GDP by the enzyme thus "flipping" the switch. GTPases play an active role in eukaryotic cells by regulating a vast array of processes, such as cell growth, cell differentiation, DNA transcription, and protein synthesis, and serve to transmit signals to downstream effectors in signaling cascades.[1−3] One of these GTPases, ras, has been the subject of much attention since its discovery in the early 1980s. The first human oncogene was found to be a GTPase that is involved in cell growth and differentiation. Since then, ras has been the target of many experimental and theoretical studies.[3−7] Despite these studies, the hydrolysis mechanism of GTP, and phosphate in general, is poorly understood and still of much interest because this reaction is generally quite slow in the absence of GTPase activating proteins. Therefore, the underlying mechanism of GTP hydrolysis, involved in all GTPases, is still an open question that is integral to understanding the roles of the specific residues involved in the enzymatic reaction within the whole super-family of GTPases, and eventually, leading to new and novel therapies for cancer.

Currently, the main mechanistic debate is focused on the hydrolysis mechanism of GTP, specifically whether it follows an associative or a dissociative pathway. In the associative pathway, formation of an intermediate or transition state with pentacoordinated phosphorus is required, whereas in the dissociative pathway, formation of a metaphosphate ion (PO_3^-) is required. Therefore, a detailed understanding of the stationary states involved in the hydrolysis process can help understand the reaction mechanism, and theoretical calculations are currently the only feasible approach available for elucidating the details of the reaction mechanism due to experimental challenges in probing the mechanism directly. During the past years, theoretical studies have shed light on the hydrolysis of GTP,

(1) Bourne, H. R.; Sanders, D. W.; McCormick, F. *Nature* **1990**, *348*, 125−132.
(2) Lowy, D. R.; Willumsen, B. M. *Rev. Biochem.* **1993**, *62*, 851−891.
(3) Sprang, S. R. *Annu. Rev. Biochem.* **1997**, *66*, 639−678.
(4) Gideon, P.; John, J.; Frech, M.; Lautwein, A.; Clark, R.; Scheffler, J. E.; Wittinghofer, A. *Mol. Cell. Biol.* **1992**, *12*, 2050−2056.
(5) Barbacid, M. *Annu. Rev. Biochem.* **1987**, *56*, 779−827.
(6) Bos, J. *Cancer Res.* **1989**, *49*, 4682−4689.
(7) Maegley, K. A.; Admiraal, S. J.; Herschlag, D. *Proc. Natl. Acad. Sci.* **1996**, *93*, 8160−8166.

catalytic activity of ras and GAP, and the effect of mutations in ras.[8−15] However, due to the computational cost, most of the ab initio and DFT quantum chemical studies related to the mechanism of GTP hydrolysis have focused on mono-phosphate esters[16−18] rather than tri-phosphate esters. In a recent theoretical study, Florian and Warshel[16] studied the nonenzymatic hydrolysis of monomethyl phosphate and explored the energetics of various reaction mechanisms using ab initio quantum mechanical calculations coupled to Langevin dipoles (LD) and polarized continuum (PCM) solvation models. Their theoretical results show that the barriers for the associative pathways are similar to those of the dissociative pathways leading the authors to assume that both are possible in aqueous solution, with the enzyme active site using either of these mechanisms depending on the particular electrostatic environment. Later, Åqvist and Warshel applied a thermodynamic analysis of the available experimental data and concluded that the evidence invoked for postulating a dissociative mechanism is equally consistent with an associative or concerted mechanism.[19] However, this conclusion was challenged by other theoretical studies. Using higher level ab initio and hybrid density functional theory methods coupled with a polarizable continuum model (PCM), Hu and Brinck[17] studied the hydrolysis mechanism of mono-phosphate mono-ester in water solution and found that the dissociative pathway is more favorable than the associative, especially when an additional water molecule is involved in the hydrolysis process. In this study, the calculated reaction barrier for the dissociative process is very close to the experimental estimate of approximately 30.7 kcal/mol (ref 20) when a water molecule is allowed to take an active role in the hydrolysis reaction. Recently, Bianciotto, et al.[18] studied the dissociative hydrolysis reaction of the mono-phosphate mono-ester in aqueous solution using PCM and explicit water models and reported a slightly different, constrained, stepwise process which includes a possible zwitterion first proposed in the late 1960s (ref 21). They suggested that previous studies had incompletely explored the reaction surface. However, the authors neither reported the charge distributions, which are critical for evaluating the presence of zwitterions, nor did they determine the fully optimized transition states corresponding to the collapse of the zwitterions, which were claimed to be rate-determining. These previous calculations may provide some insight into the tri-phosphate hydrolysis mechanism. However, explicitly studying tri-phosphate hydrolysis is the only definitive path to fully understanding the process involved in GTPases such as ras.

Here, we assume that details of the hydrolysis of the mono-phosphate anion can serve as a guide to the basic computational approach to understanding the hydrolysis of GTP, but subtle and fundamental details of the hydrolysis mechanism of GTP, especially whether the mechanism is associative or dissociative, will not be accurately modeled by the mono-phosphate ester. Chemically speaking, the hydrolysis pathways of mono-phosphate esters and tri-phosphate esters in aqueous solution may be similar but the reaction energetics, which are critical to analyze the preference for associative vs dissociative pathways, of the two systems are probably different, with tri-phosphate probably more sensitive to polar solvents such as water. Studying the hydrolysis of the tri-phosphate ester should provide a more direct clue to accurately understanding GTP hydrolysis. Therefore, the main aim of this work is to study the hydrolysis mechanism of both the tri-phosphate ester, which is taken as a model of GTP in this work, and mono-phosphate ester at the same theoretical level. It is our goal to use these results to better understand the hydrolysis mechanism of GTP in solution and ultimately in GTPase enzymes.

As far as we know, there are neither direct experimental data nor independent theoretical results on the hydrolysis of tri-phosphate mono-ester in aqueous solution. The only relevant experimental evidence comes from tri-phosphate ($H_5P_3O_{10}$). On the basis of studies of the hydrolysis of tri-phosphate from detergents in a rural wastewater system, Halliwell et al. estimated the activation energy for P−O bond cleavage to be 30.8 kcal/mol.[22] Van Wazer estimated that the activation energy for the hydrolysis of tri-phosphate at pH = 7 and 30 °C is appropriately 29 kcal/mol.[23]

To validate the computational approach, we first studied the hydrolysis of mono-phopshate methyl ester, which has already been studied by other groups at different theoretical levels and compared our results with the experimental data and previous calculations. The overall agreement of our results (32.3 kcal/mol in Table 1) with the experimental data (30.7 kcal/mol in Table 1) suggests that the method yields results within reasonable chemical accuracy (<2 kcal/mol) for mono phosphate ester in our studies. Extensive studies of the tri-phosphate ester hydrolysis, including changes in charge distribution and the effects of the environmental dielectric constant on the energetics of the reaction, were carried out using the same methodologies. Our results for the energy barrier of tri-phosphate hydrolysis (30.4 kcal/mol) are in good agreement with the previously discussed relevant experimental data. However, it should be noted that despite the success of the approach used for mono-phosphate hydrolysis, there is no guarantee that application of the same methods to the tri-phosphate hydrolysis would give the same energy deviation (less than 2 kcal/mol). Current solvation models are not well parametrized for multiply charged anions. It is known that these models can produce large errors in absolute solvation energies of negatively charged ions in water.[24−26] However, based on previously published results,[16]

(8) Langen, R.; Schweins, T.; Warshel, A. *Biochem*. **1992**, *31*, 8691−8696; Schweins, T.; Langen, R.; Warshel, A. *Struct. Biol*. **1994**, *1*, 476−484; Schweins, T.; Warshel, A. *Biochem*. **1996**, *35*, 14 232−14 243; Schweins, T.; Geyer, M.; Kalbitzer, H. R.; Wittinghoger, A.; Warshel, A.; *Biochem*. **1996**, *35*, 14 225−14 231.
(9) Kinoshita, H.; Shimizu, K. *Bioorg. Med. Chem. Lett.* **1998**, 1083−1088.
(10) Futatsugi, N.; Hata, M.; Hoshino, T.; Tsuda, M. *Biophys. J*. **1999**, *77*, 3287−3292; Futatsugi, N.; Tsuda, M. *Biophys. J*. **2001**, *81*, 3483−3488.
(11) Ma, J.; Karplus, M. *Proc. Natl. Acad. Sci*. **1997**, *94*, 11 905−11 910.
(12) Allin, C.; Ahmadian, M. R.; Wittinghofer, A.; Gerwert, K. *Proc. Natl. Acad. Sci*. **2001**, *98*, 7754−7759.
(13) Glennon, T. M.; Villa, J.; Warshel, A. *Biochem*. **2000**, *39*, 9641−9651.
(14) Resat, H.; Straastma, T. P.; Dixon, D. A.; Miller, J. H. *Proc. Natl. Acad. Sci*. **2001**, *98*, 6033−6038.
(15) Cavalli, A.; Carloni, P. *J. Am. Chem. Soc*. **2002**, *124*, 3763−3768.
(16) Florian J.; Warshel, A. *J. Phys. Chem. B* **1998**, *102*, 719−734.
(17) Hu, CH−H.; Brinck, T. *J. Phys. Chem. A* **1999**, *103*, 5379−5386.
(18) Bianciotto, M.; Barthelat, J.; Vigroux, A. *J. Am. Chem. Soc*. **2002**, *124*, 7573−7587; Bianciotto, M.; Barthelat, J.; Vigroux, A. *J. Phys. Chem. A*. **2002**, *106*, 6521−6526.
(19) Åqvist, J.; Kolmodin, K.; Florain, J.; Warshel, A. *Chem. Biol*. **1999**, *6*, 71−80.
(20) Bunton, C. A.; Llewellyn, D. R.; Oldham, K. G.; Vernon, C. A. *J. Chem. Soc*. **1958**, 3574.
(21) Jencks, W. P. *Catal. Chem. Enzymol.* **1987**.
(22) Halliwell, D. J.; Mckelvie, I. D.; Hart, B. T.; Dunhill, R. H. *Wat. Res.* **2001**, *35*, 448−454.
(23) Van Wazer, J. R.; Griffith, E. J.; McCullough, J. F. *J. Am. Chem. Soc.* **1955**, *77*, 287−291.
(24) Florian J.; Warshel A. *J. Phys. Chem. B* **1997**, *101*, 5583−5595
(25) Li, J.; Zhu, T.; Cramer, C. J.; Truhlar, D. G. *J. Phys. Chem. A* **2000**, *104*, 2178−2182.

Table 1. Relative Energies (kcal/mol) of the Stationary Species of the Reaction: $[MeOPO_3H]^- + H_2O$ and $[MeOPO_3]^{2-} + H_2O$[a]

	B3LYP/6-31+G(d,p)				B3LYP/cc-PVTZ+//B3LYP/6-31+G(d,p)				MP2/6-31+G(d,p)//B3LYP/6-31+G(d)[17]	MP2/6-31+G(d,p)//HF/6-31G(d)[16]	CCSD(T)/(G2X)//B3LYP/6-31+G(d)[17]
	ΔE_g	ΔG_g	ΔG_{solv}	ΔG_{aq}	ΔE_g	ΔG_g	ΔG_{solv}	ΔG_{aq}	ΔG_{aq}	ΔG_{aq}	ΔG_{aq}
					associative of $[MeOPO_3H]^- + H_2O$						
reactant-complex	0.0	0.0	−71.7	0.0	0.0	0.0	−69.2	0.0			
A_TS1	40.1	40.5	−74.9	37.2	40.8	40.8	−72.2	37.8	36.1	34.5	37.5
INT	30.6	33.7	−73.1	32.3	31.7	34.8	−70.2	33.8			
A_TS2	39.0	38.6	−72.7	37.5	39.4	39.0	−69.7	38.4	37.6	38.3	38.6
					dissociative of $[CH_3PO_4H]^- + H_2O$						
D_TS_a	33.1	30.3	−67.3	34.6	34.9	32.1	−65.3	35.9	33.4	33.6	
D_TS_b	26.6	25.2	−74.8	22.1	28.6	27.3	−72.5	24.0	23.8		28.4
D_INT	13.3	9.4	−66.4	14.6	14.1	10.2	−63.7	15.7			
D_TS_C	35.5	31.1	−71.5	31.3	36.4	32.0	−68.9	32.3	33.1		
					$[MeOPO_3]^{2-} + H_2O$						
reactant-complex	0.0	0.0	−229.9	0.0	0.0	0.0	−227.6	0.0			
A_TS	51.7	48.0	−236.5	41.5	49.7	46.0	−231.8	41.8		42.7	
exp	30.7 [20]										

[a] $\Delta G_g = \Delta E_g + \Delta\Delta G_g$; $\Delta G_{aq} = \Delta G_g + \Delta\Delta G_{solv}$; $\Delta\Delta G_g$, thermal correction to gibbs free energy; ΔG_{solv}, solvation energy; ΔG was calculated at $T =$ 298.15 K.

we expect the methodology to yield reasonable relative solvation and activation energies (within 4 kcal/mol uncertainty) for tri-phosphate anions where the conformations are very similar in geometries and electronic structure.

In the GTP bound state of enzymes, such as ras, it is not certain whether GTP ($P_\gamma O_3$) is protonated or un-protonated in the active site, but it is likely that the $P_\gamma O_3$ abstracts a proton from a nearby water or one of the residues conserved in the GTPase superfamily. Therefore, we assume the protonated form of the tri-phosphate throughout this work.

Methods and Computation Details

All the geometric structures of the reactant complexes, intermediate states, and transition states in the hydrolysis pathways were fully optimized in gas phase using the hybrid density functional method B3LYP[27−29] with the 6-31+G(d,p) basis set, except for where specifically noted otherwise. Minima and transition states were further verified by vibrational frequency analysis at the same theoretical level. Intrinsic reaction coordinate (IRC) calculations were performed, and the reaction paths connecting reactant complexes, transition states, intermediate states, and product complexes were explored.[30,31] The path was computed in mass-weighted internal coordinates in steps of 0.1 amu$^{1/2}$ bohr by using Gonzales and Schlegel's method.[32,33] After the stationary points, reactant complexes, transition states, and intermediate states had been located and the reaction paths clarified, corresponding single point energy calculations of all the stationary species were then carried out using the cc-PVTZ+ [34−37] basis set in a model for aqueous solution at the 6-31+G(d,p) optimized geometries. Although the reaction barriers are underestimated for certain types of reactions, DFT methods are currently the most popular method for macromolecular calculations due to the computational accuracy at relatively low computational cost.[38,39]

All of the solvation energies were determined by using the self-consistent reaction field (SCRF) method combined with a Poisson−Boltzmann solver coded in JAGUAR,[40−42] except for where specifically noted otherwise. The practical implementation of SCRF involves the synthesis of a polarizable quantum mechanical solute and a continuum description of the solvent. First, the gas-phase electron density for the solute is determined and the resulting charge distribution is used to calculate atom-centered charges via an electrostatic potential (ESP) least-squares fitting procedure. The gas-phase ESP charges are then passed to a Poisson−Boltzmann (PB) equation solver along with the van der Waals radii for each atom.[42] The radii are used to determine a solvent accessible surface, which defines the solute/solvent boundary. The interior solute region is assigned a dielectric constant of 1 and the exterior solvent region is assigned a dielectric of 80 for bulk water. The PB solver computes the charge distribution at the solute−solvent interface, which is then used to compute the solute−solvent part of the Hamiltonian. The interaction polarizes the solute and a new ESP charge distribution is then calculated and passed to the PB solver. The calculations are repeated until convergence is reached. In this model, the entire solute ESP charge was placed inside the solute cavity. Although some penetration of charges outside the cavity is unavoidable, especially for negatively charged ions, this approximation has been shown to yield quite good results.[43−47] To evaluate the sensitivity of our results to the atomic radii used in the calculations, especially for tri-phosphate anion, we repeated the solvation calculations using the PCM model coded in Gaussian 98 program with Pauling's atomic radii multiplied by a standard factor of 1.2, used by previous studies.[16−18]

(26) Chambers, C. C.; Hawkins, G. D.; Cramer, C. J.; Truhlar, D. G. *J. Phys. Chem.* **1996**, *100*, 16 385−16 398.
(27) Becke, A. D. *J. Chem. Phys.* **1993**, *98*, 5648.
(28) Lee, C.; Yang, W.; Parr, R. G. *Phys. Rev. B* **1988**, *37*, 785.
(29) Stevens, P. J.; Devlin, F. J.; Chabalowski, C. F.; Frisch, M. J. *J. Phys. Chem.* **1994**, *98*, 11 623.
(30) Fukui, K. *J. Phys. Chem.* **1970**, *74*, 4161.
(31) Fukui, K. *Acc. Chem. Res.* **1981**, *14*, 363.
(32) Gonzalez, C.; Schlegel, H. B. *J. Chem. Phys.* **1989**, *90*, 2154.
(33) Gonzalez, C.; Schlegel, H. B. *J. Phys. Chem.* **1990**, *94*, 5523.
(34) Dunning, T. H.; Jr. *J. Chem. Phys.* **1989**, *90*, 1007.
(35) Kendall, R. A.; Dunning, T. H.; Jr.; Harrison, R. J. *J. Chem. Phys.* **1992**, *96*, 6796.
(36) Woon, D. E.; Dunning, T. H.; Jr. *J. Chem. Phys.* **1993**, *98*, 1358.
(37) Woon, D. E.; Peterson, K. A.; Dunning, T. H., Jr.; unpublished.
(38) Siegbahn, P. E. M.; Blomberg, M. R. A. *Annu. Rev. Phys. Chem.* **1999**, *50*, 221.
(39) Siegbahn, P. E. M.; Blomberg, M. R. A. *Chem. Rev.* **2000**, *100*, 421; Blomberg, M. R. A. and Siegbahn, P. E. M. *J. Phys. Chem. B* **2001**, *39*, 9375−9386.
(40) Jaguar 4.1; Schroedinger, Inc. Portland, OR, 2001.
(41) Tannor, D. J.; Marten, B.; Murphy, R.; Friesner, R. A.; Stikoff, D.; Nicholls, A.; Ringnalda, M.; Goddard III, W. A.; Honig, B. *J. Am. Chem. Soc.* **1994**, *116*, 11 875.
(42) Marten, B.; Kim, K.; Cortis, C.; Friesner, R. A.; Murphy, R. B.; Ringnalda, M. N.; Sitkoff, D.; Honig, B. *J. Phys. Chem.* **1996**, *100*, 11 775.
(43) Bachs, M.; Luque, F. J.; Orozco, M. *J. Comput. Chem.* **1994**, *15*, 446.
(44) Marten, B.; Kim, K.; Cortis, C.; Friesner, R. A.; Murphy, R. B.; Ringnalda, M. N.; Sitkoff, D.; Honig, B. *J. Phys. Chem.* **1996**, *100*, 11 775.
(45) Rashin, A. A.; Young, L.; Topol, I. A. *Biophys. Chem.* **1994**, *51*, 359.
(46) Corcelli, S. A.; Kress, J. D.; Pratt, L. R.; Tawa, G. J. Pacific Symosium on Biocomputing '96; World Scientific: NJ, 1995; p 143.
(47) Topol, I. A.; Tawa, G. J.; Caldwell, R. A.; Eissenstat, M. A.; Burt, S. K. *J. Phys. Chem. A.* **2000**, *104*, 9619−9624.

The results were very similar to those obtained using the JAGUAR program (see Table S2−4).

All the gas-phase calculations were carried out with the Gaussian 98 program,[48] whereas all the aqueous solution optimizations were performed using the JAGUAR code.

Results

1. Reaction of $[MeOPO_3H]^- + H_2O$ and $[MeOPO_3]^{2-} + H_2O$. For the protonated mono-phosphate methyl ester $[MeOPO_3H]^-$, both the associative and dissociative hydrolysis pathways were studied. The structures of the calculated stationary species involved in the hydrolysis are shown in Figure 1, and a comparison of the corresponding energetics of the stationary states with previous theoretical and experimental data are listed in Table 1. For the associative mechanism pathway, $[MeOPO_3H]^-$ first abstracts a proton from the nucleophilic water molecule leading to the first transition state (A_TS1 in Figure 1a), and then forms the intermediate state INT as the OH^- group attacks the phosphorus. The P−O5 bond is extended as the proton, H1, shifts to the bridge oxygen, O5, and finally broken at the second transition state (A_TS2 in Figure 1a). For the dissociative pathway, the P−O5 bond can be broken through either intramolecular proton transfer (D_TS_a in Figure 1a) or intermolecular proton transfer (D_TS_b in Figure 1a) to form an intermediate complex (D_INT) of PO_3^-, water and methanol. The PO_3^- fragment then further reacts with water to form $H_2PO_4^-$ (D) via the transition state D_TS_c. Our results show that the activation energy of D_TS_a (36.0 kcal/mol) is very close to those of A_TS1 (37.8 kcal/mol) and A_TS2 (38.4 kcal/mol) in aqueous solution, whereas the energy of D_TS_b (24.0 kcal/mol) is much lower due to the participation of a "bridge" water molecule.

Our energy barriers for the associative hydrolysis process, A_TS1 and A_TS2, are very close to the previous theoretical results of 36.1 and 37.6 kcal/mol obtained using MP2/6-31+G(d,p)//B3LYP/6-31+G(d), and 37.5 and 38.6 kcal/mol obtained using CCSD(T)/(G2X)//B3LYP/6-31+G(d)[17](see Table 1). Our energy barriers for the dissociative hydrolysis process, D_TS_a (35.9 kcal/mol) and D_TS_b (24.0 kcal/mol), are also very close to the corresponding results (33.4 and 23.8 kcal/mol, respectively) of MP2/6-31+G(d,p)//B3LYP/6-31+G(d) calculations,[17] but the energy of D_TS_b is ca. 4 kcal/mol lower than the corresponding results of CCSD(T)/(G2X)//B3LYP/6-31+G(d) (28.4 kcal/mol)[17](see Table 1). Our result for D_TS_c is 32.3 kcal/mol, very close to the result of MP2/6-31+G(d,p)//B3LYP/6-31+G(d) calculations (33.1 kcal/mol)[17] and Bianciotto et al.'s result, 31.0 kcal/mol.[18]

For the unprotonated mono-phosphate methyl ester $[MeOPO_3]^{2-}$, only the associative hydrolysis pathway was studied because there is no proton on the phosphate that can be transferred to initiate the dissociative mechanism (see Figure 1b). Only one concerted transition state A_TS was found (shown in Figure 1b) corresponding to activation energy of 41.8 kcal/mol (Table 1), which is very close to the previous theoretical result of 42.7 kcal/mol[16] (Table 1). The free energy of A_TS is ca. 3 kcal/mol higher than that of A_TS2 (Figure 1a) and 18 kcal/mol higher than that of D_TS_b (Figure 1a) for the protonated species $[MeOPO_3H]^-$.

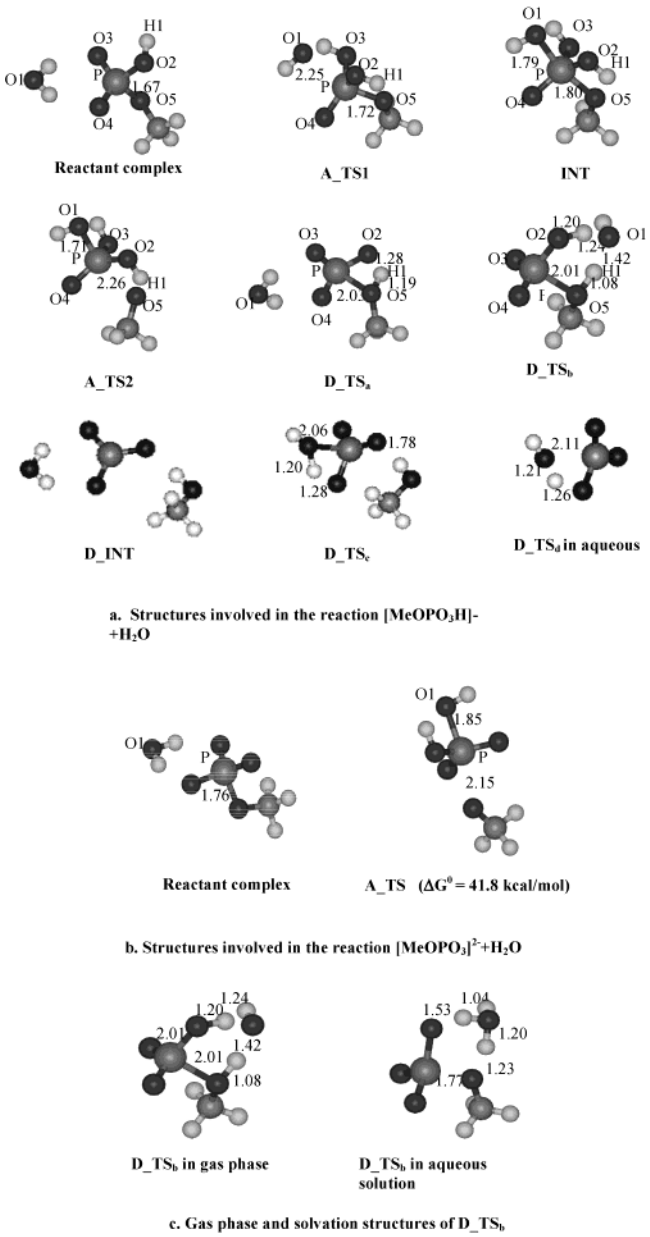

Figure 1. Structures of the stationary species involved in reactions: $[MeOPO_3H]^- + H_2O$ (Figure 1.a) and $[MeOPO_3]^{2-} + H_2O$ (Figure 1.b).

To explore the effects of solvation on the hydrolysis of the protonated monomethyl ester, we fully optimized the stationary structures in a dielectric of 80. Table 2 shows the dielectric effect on the geometry RMS and energetics. The optimization in dielectric field did not significantly change the geometries of the stationary species and resulted in a 0.3 Å maximum RMS for the stationary species, and no significant change in the relative energetics of the transition states and intermediate states. During the calculations we found that in contrast to the other stationary species, D_TS_b is very sensitive to aqueous solvent. The electronic distribution of D_TS_b in gas phase is significantly

(48) Frish, M. J.; Trucks, G. W.; Schlegel, H. B.; Scuseria, G. E.; Robb, M. A.; Cheeseman, J. R.; Zakrzewski, V. G.; Montgomery, J. A.; Jr.; Stratmann, R. E.; Burant, J. C.; Dapprich, S.; Millam, J. M.; Daniels, A. D.; Kudin, K. N.; Strian, M. C.; Farkas, O.; Tomas, J.; Barone, V.; Cossi, M.; Cammi, R.; Mennucci, B.; Pomelli, C.; Adamo, C.; Clifford, S.; Ochterski, J.; Petersson, G. A.; Ayala, P. Y.; Cui, P. Y.; Morokuma, K.; Malick, D. K.; Rabuck, A. D.; Raghavachari, K.; Foresman, J. B.; Cioslowski, J.; Ortiz, J. V.; Baboul, A. G.; Stefanov, B. B.; Liu, G.; Liashenko, A.; Piskorz, P.; Komaromi, I.; Gomperts, R.; Martin, R. L.; Fox, D. J.; Keith, T.; Al-Laham, M. A.; Peng, C. Y.; Nanayakkara, A.; Gonzalez, C.; Challacombe, M.; Gill, P. M. W.; Johnson, B.; Chen, W.; Wong, M. W.; Andres, J. L.; Gonzalez, C.; Head-Gordon, M.; Replogle, E. S.; Pople, J. A. Gaussian 98 Revision A.7, Gaussian, Inc., Pittsburgh, PA, 1998.

Table 2. Solvent Effect on the Geometry Structure and Free Energy (kcal/mol) of the Reaction: $[MeOPO_3H]^- + H_2O$

	A_TS1	INT	A_TS2	D_TS$_a$	D_TS$_b$	D_TS$_c$
Opt + SP in gas	40.8	34.8	39.0	32.1	27.3	32.0
Opt in gas & SP in water	37.8	33.8	38.4	36.0	24.0	32.3
Opt & SP in water	37.3	31.5	39.2	36.2	21.8[a]	33.5[a]
RMS(Å) (gas vs aqueous)	0.1	0.1	0.3	0.3	0.2	0.1(D_TS$_d$)

[a] See ref 50.

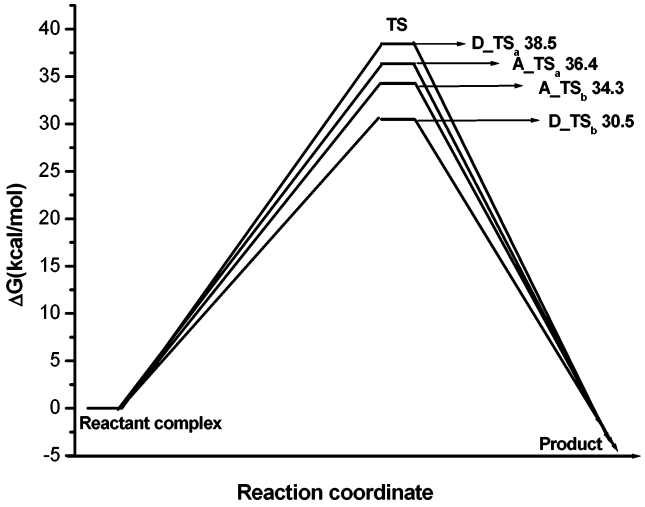

Figure 2. Energy profiles of the reaction: $TME(H)^{3-} + H_2O$ in aqueous.

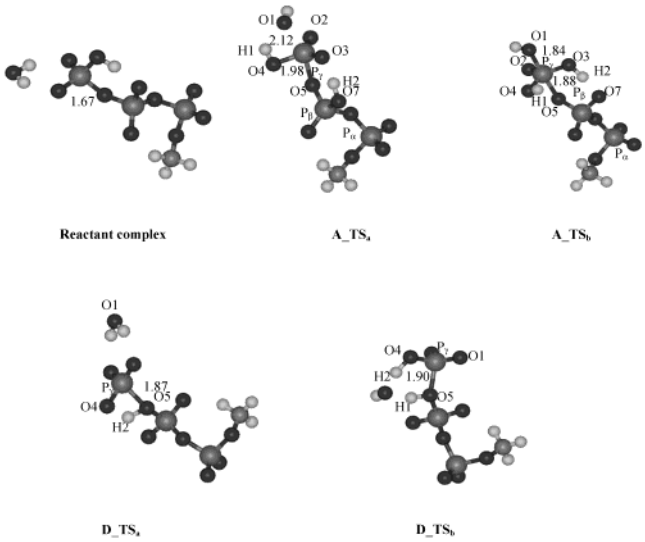

Figure 3. Gas-phase structures of the stationary species involved in the reaction: $TME(H)^{3-} + H_2O$.

changed in the dielectric field although the RMS geometry difference is only 0.2 Å. In gas phase, D_TS$_b$ exists as $[HPO_3$-$HOCH_3]$ and OH^- (Figure 1c), whereas in aqueous solution it exists as an $[PO_3OCH_3]^{2-}$ and H_3O^+ ionic pair (Figure 1c) which should be significantly stabilized by aqueous solution.

2. Reaction of the Hydrolysis of Protonated Tri-Phosphate Methyl Ester (TME): TME(H)$^{3-}$+H$_2$O. The energy profiles and structures corresponding to the reactant complex and transition states for the associative and dissociative pathways for the hydrolysis of protonated TME are shown in Figure 2 and Figure 3, respectively. Two possible associative hydrolysis pathways, which are both concerted with only one transition state each, were found. The main geometrical difference between the transition states of the two associative pathways, A_TS$_a$ and A_TS$_b$, are the positions of H1 and H2, and the O1−P$_\gamma$ distance. In A_TS$_a$, the H1−O4 bond is perpendicular to the P$_\gamma$O$_3$ (P$_\gamma$−O$_2$−O$_3$−O$_4$) plane, whereas it is in the P$_\gamma$O$_3$ plane in A_TS$_b$. H2 is transferred from O3 to O7 in A_TS$_a$ but not in A_TS$_b$. The distances of O1−P$_\gamma$ and O5−P$_\gamma$ of A_TS$_a$ are 2.12 Å and 1.98 Å, whereas the corresponding distances of A_TS$_b$ are 1.84 and 1.88 Å, respectively.

Table 3. Relative Energies (kcal/mol) of the Stationary Species of Reaction: $TME(H)^{3-} + H_2O$

	B3LYP/6-31+G(d,p)				B3LYP/cc-PVTZ+// B3LYP/6-31+G(d,p)			
	ΔE_g	ΔG_g	ΔG_{solv}	ΔG_{aq}	ΔE_g	ΔG_g	ΔG_{solv}	ΔG_{aq}
associative								
reactant-complex	0.0	0.0	−374.79	0.0	0.0	0.0	−371.47	0.0
A_TS$_a$	47.1	46.9	−386.8	34.8	47.3	47.2	−382.3	36.4
A_TS$_b$	54.5	54.2	−396.7	32.3	54.8	54.5	−391.7	34.3
dissociative								
D_TS$_a$	39.3	35.1	−372.8	37.2	41.3	37.1	−370.2	38.5
D_TS$_b$	39.7	36.1	−382.5	28.4	42.0	38.5	−379.5	30.5

In the gas phase, the free energy of A_TS$_a$ (47.2 kcal/mol) is lower than A_TS$_b$ (54.5 kcal/mol), whereas in aqueous solution the free energy of A_TS$_a$ (36.4 kcal/mol) is ca. 2 kcal/mol higher than that of A_TS$_b$ (34.3 kcal/mol).

For the dissociative pathway, both intramolecular and intermolecular proton transfer processes were studied. In the intramolecular pathway proton H2 transfers to the bridge oxygen O5, leading directly to the dissociation of the P$_\gamma$−O$_5$ bond (D_TS$_a$ shown in Figure 3). In contrast, the intermolecular proton-transfer proceeds through an active water "bridge" (D_TS$_b$). The P$_\gamma$−O$_5$ bond length in D_TS$_a$ (1.87 Å) and D_TS$_b$ (1.90 Å) is nearly identical.

In the gas phase the free energy of D_TS$_a$ (37.1 kcal/mol) and D_TS$_b$ (38.5 kcal/mol) are very close, but in the aqueous solution the free energy of D_TS$_b$ is ca. 8 kcal/mol (Table 3) lower than D_TS$_a$ due to the involvement of the bridge water molecule.

Unlike the mono-phosphate energetics the associative (34.3 kcal/mol) and dissociative (30.5 kcal/mol) reaction barriers for $TME(H)^{3-} + H_2O$ are quite close in aqueous solution, although the free energy of the dissociative transition state (36.1 kcal/mol) is much lower than that of the associative transition state (54.2 kcal/mol) in the gas phase. Due to uncertainties in solvation energy calculations for such large negatively charged systems, we are unable to definitively conclude that the tri-phosphate ester prefers the dissociative hydrolysis pathway rather than the associative pathway, as in the mono-phosphate case. It is probably more reasonable to say that both pathways are possible alternatives, and the enzyme modulates the mechanisms depending on the local environment.

3. Reaction of TME(H)$^{3-}$ + 2H$_2$O. The structures of the stationary states involved in the reaction of $TME(H)^{3-} + 2H_2O$ are shown in Figure 4, and the energy profile in aqueous solution is displayed in Figure 5. There are several possible pathways corresponding to the associative mechanism, and three were analyzed in this work (see Figure 5). Unlike the previous reaction of $TME(H)^{3-} + H_2O$, which is a concerted process, $TME(H)^{3-} + 2H_2O$ is a stepwise process with at least two transition states. The reactant complex, first transition state (A_TS1), and the first associative intermediate state (A_INT1) are common to all three of the pathways explored. With a

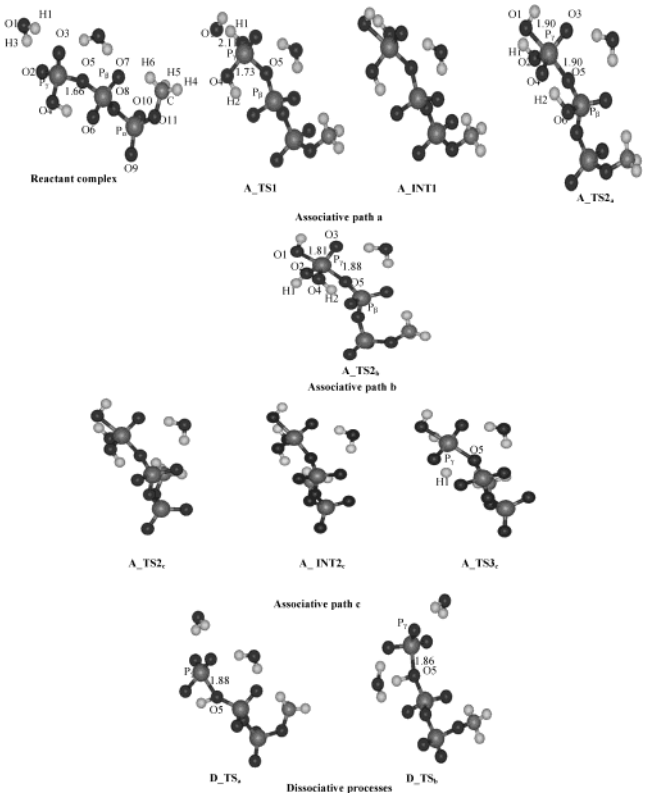

Figure 4. Gas-phase structures of the stationary species involved in the reaction: $TME(H)^{3-} + 2H_2O$.

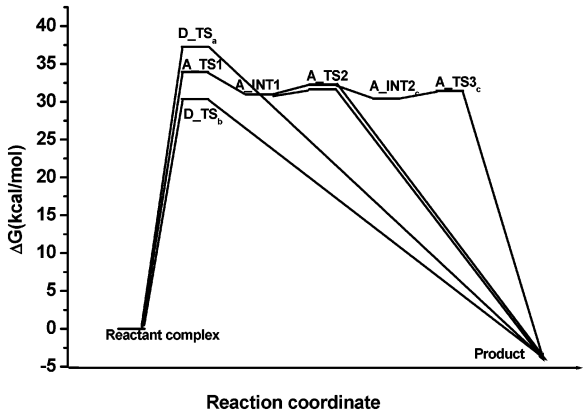

Figure 5. Energy profiles of the reaction: $TME(H)^{3-} + 2H_2O$ in aqueous.

common characteristic the proton transfer from the attacking water to an oxygen atom of γ phosphate, A_TS1 is the rate determining step in all three of the pathways (see Table 4). The bond lengths of O1−P_γ and O5−P_γ are 2.11 and 1.73 Å in the first transition state. The three associative pathways diverge at the second transition state. In associative path a, the second transition state, A_TS2_a, is related to the shift of proton H2 from O4 to O6, in concert with the bond extension of O5−P_γ. The bond lengths of O1−P_γ and O5−P_γ are both ca. 1.9 Å in A_TS2_a. In contrast, the second transition state of associative path b (A_TS2_b), corresponds to rotation of the proton H1 toward a P_β oxygen (O4). Path c involves a complicated conformational change of the methyl group and is probably impossible to be realized in the active site of GTPases.

For the dissociative process, the intramolecular (D_TS_a in Figure 4) and intermolecular (D_TS_b in Figure 4) transition states are similar to the corresponding transition states of the reaction $GTP(H)^{3-}+H_2O$. The bond length of O5−P_γ in D_TS_a and D_TS_b is 1.88 and 1.86 Å, respectively.

In the gas phase, the activation energy of the dissociative pathways (D_TS_a and D_TS_b) is much lower than that of associative pathways (see Table 4). While in aqueous solution, the free energy of D_TS_b (intermolecular proton-transfer pathway) is 3.5 kcal/mol lower than that of A_TS1, and the energy barrier of the intramolecular proton-transfer pathway (D_TS_a) is 3.4 kcal/mol higher than A_TS1. Compared to the reaction of $GTP(H)^{3-} + H_2O$, the energy barrier of the reaction $GTP(H)^{-3} + 2H_2O$ was not significantly changed, with the difference between the associative and dissociative transition states remaining less than 4 kcal/mol. This again is close enough to assume that both mechanisms are possible in aqueous solution.

Table 4. Relative Energies (kcal/mol) of the Stationary Species of Reaction: $Tme(H)^{3-} + 2H_2O$

	B3LYP/6-31+G(d,p)				B3LYP/cc-PVTZ+//B3LYP/6-31+G(d,p)			
	ΔE_g	ΔG_g	ΔG_{solv}	ΔG_{aq}	ΔE_g	ΔG_g	ΔG_{solv}	ΔG_{aq}
associative								
reactant-complex	0.0	0.0	−361.62	0.0	0.0	0.0	−358.12	0.0
A_TS1	44.4	45.7	−374.5	32.9	44.3	45.6	−369.8	33.9
INT	44.2	45.8	−377.9	29.5	44.5	46.1	−373.2	31.0
A_TS2_a	46.1	45.4	−377.8	29.2	47.2	46.5	−372.9	31.7
A_TS2_b	52.0	52.0	−383.5	30.1	52.6	52.7	−378.6	32.2
A_TS2_c	45.5	48.4	−378.0	32.3	44.5	47.4	−373.2	32.3
INT2	45.1	46.6	−379.3	28.9	46.1	47.5	−375.2	30.4
A_TS3	46.6	46.2	−378.8	29.0	48.1	47.7	−374.3	31.5
dissociative								
D_TS_a	40.6	36.4	−362.2	35.8	42.6	38.4	−359.3	37.3
D_TS_b	40.7	37.4	−370.3	28.7	43.4	39.2	−367.0	30.4

Table 5. Charge Distribution on the Stable States of Reaction: $TME(H)^{3-} + 2H_2O$

	$P_\gamma O_3$	$P_\beta O_3$	$P_\alpha O_3$	OCH_3	ΔG_{solv}
reactant-complex	−1.145	−0.966	−0.928	−0.291	−358.1
A_TS1	−0.844	−1.051	−0.936	−0.285	−369.8
INT1	−0.922	−1.079	−0.953	−0.289	−373.2
A_TS2_a	−0.986	−1.007	−0.977	−0.294	−372.9
A_TS2_b	−0.880	−1.173	−0.980	−0.289	−378.6
A_TS2_c	−0.994	−0.969	−0.938	−0.332	−373.9
INT2	−0.937	−1.067	−0.937	−0.321	−375.2
A_TS3	−1.000	−1.026	−0.960	−0.305	−374.3
D_TS_a	−1.144	−0.917	−0.943	−0.313	−359.3
D_TS_b	−1.243	−0.926	−0.956	−0.309	−367.0

4. Charge Distribution on TME. We analyzed charge distributions for two different models of the TME hydrolysis (TME with one water molecule and two water molecules). Both give similar results so we focus our discussion on the distribution for the most representative model, one that includes two water molecules. We investigated the charge distributions of the stationary species of the reaction $TME(H)^{3-} + 2H_2O$ by dividing the system into four parts $P_\gamma O_3$ (P_γ−O2−O3−O4), $P_\beta O_3$ (P_β−O5−O6−O7), $P_\alpha O_3$ (P_α−O8−O9−O10) and OCH_3 (O11−C−H4−H5−H6) (see reactant complex of Figure 4, path a). In the reactant complex, the main charge buildup is located on the $P_\gamma O_3$ group (see Table 5, column1). In the transition state A_TS1, however, the main charge buildup is shifted to the $P_\beta O_3$ group through the bridging ester oxygen (see Table 5 column2). This analysis clearly shows that negative charge shifts from $P_\gamma O_3$ to $P_\beta O_3$ in the associative hydrolysis processes. This result agrees with the recent experimental result that suggests that ras

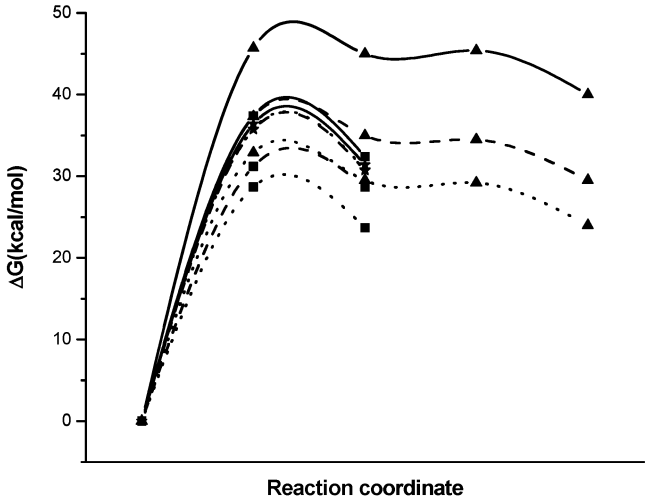

Figure 6. Effect of environmental dielectric constant on the energetics of the reaction: $TME(H)^{3-} + 2H_2O$. ▲, associative path a; ★, dissociative a; ■, dissociative b. Solid lines, gas phase ($\epsilon = 1$); dash lines, a model of the protein environment ($\epsilon = 4$); dotted lines, bulk water solution ($\epsilon = 80$).

catalyzes GTP hydrolysis by shifting negative charge from the γ- to β-phosphate.[51] In contrast, this charge-transfer process was not found in the dissociative hydrolysis process of our model.

5. Effect of Environmental Dielectric Constant. To explain the effect of the dielectric constant on the energy of hydrolysis in our model for GTP, we calculated the energy for the stationary points of hydrolysis of $TME(H)^{3-}$ with two water molecules ($TME(H)^{3-} + 2H_2O$) in different dielectric environments. The results are displayed in Figure 6. In Figure 6, the associative path a is shown by ▲, whereas dissociative a and dissociative b are shown by ★ and ■, respectively. Solid lines represent the gas phase ($\epsilon = 1$), dash lines for a model of the protein environment ($\epsilon = 4$), and dotted lines correspond to bulk water solution ($\epsilon = 80$). It can be seen that the dielectric environment influences the energetics of the associative and dissociative b pathways dramatically. The activation energy of A_TS1 is reduced by 8.4 and 12.8 kcal/mol for $\epsilon = 4$ and $\epsilon = 80$, respectively. The activation energy of D_TS_b is reduced by 6.2 and 8.7 kcal/mol in $\epsilon = 4$ and $\epsilon = 80$ environment, respectively. In contrast, the energetics of dissociative hydrolysis pathway a proceeding via the intramolecular proton transfer is not significantly influenced (ca. 0.7 kcal/mol) by the dielectric model.

Discussion

For mono-phosphate mono-ester, participation of an additional water molecule in the dissociative hydrolysis process is critical for evaluating the hydrolysis mechanism, and it is the source of the debate between Florian and Warshel,[16] who did not account for additional water participation, and Hu and Brinck,[17] who argue that additional water molecules actively participate and play an important role in the hydrolysis process, especially dissociative process. Our results agree with Hu and Brink and suggest that an additional water molecule participates in the dissociative hydrolysis process. As our results show, without the participation of an additional explicit water molecule, the activation barriers for the associative and dissociative pathways are very close in aqueous solution, though the energy of the dissociative transition state is much lower than that of the associative transition state in gas phase. Participation of an additional explicit water molecule, acting as a bridge in the proton transfer process, significantly reduces the energy barrier of P−O bond cleavage of the dissociative hydrolysis pathway, and the following reaction $PO_3^- + H_2O$ hence becomes the rate determining step in this process. Our energy barrier for the reaction $PO_3^- + H_2O$ is 32.3 kcal/mol, which is very close to the experimental data 30.7 kcal/mol. Our results suggest that the mono-phosphate mono-ester favors the dissociative hydrolysis mechanism.

Generally, continuum models are adequate to describe reactions in solution and they do not significantly change the geometries of solutes. However, as it was documented in ref 49, current continuum models may not be reliable when solvent molecules are directly involved in the reaction pathway, such as in our dissociative pathway b (D_TS_b) which involves an explicit water molecule in the proton transfer. Although the RMS deviation is only 0.2 Å, the electronic distribution is significantly changed and this change may result in significant stabilization in the continuum solvation model. This point has been extensively addressed by Bianciotto et al.[18] for the mono-phosphate case. Bianciotto et al. showed that in cases where the PCM model tends to fail, such as the transition state D_TS_b, explicit water molecules could serve as a good model for the general effects of solvent on the reaction pathway. We have repeated their calculations (unpublished) and our results support the suggestion that 3 or 4 explicit water molecules simulate the effect of PCM models quite well in the phosphate hydrolysis reactions studied here.

In ref 18, Bianciotto et al. claimed that proton transfer and P−O bond cleavage for the reaction of $[MeOPO_3H]^- + H_2O$ become uncoupled in aqueous solution although they are concerted in gas phase as we and other groups have found, and there exists an anionic zwitterion $MeO^+(H)PO_3^{2-}\cdot H_2O$ as a key intermediate between the first transition state corresponding to the proton transfer and the second transition state corresponding to the P−O bond cleavage. They also assumed that the collapse (via P−O bond cleavage) of the zwitterion form $MeO^+(H)PO_3^{2-}\cdot H_2O$ is rate determining. However, their full geometry optimizations of the transition structures for the collapse of anionic zwitterions failed. To determine the charge character of the proposed zwitterions in the hydrolysis of phosphate ester, we studied the hydrolysis of mono-phosphate monoester using PCM model coded in Gaussian98, SCRF model coded in Jaguar and explicit water molecules. We then extensively analyzed the

(49) Cramer, C. J.; Truhlar, D. G. *Chem. Rev.* **1999**, *99*, 2161.
(50) (a) The structure of D_TS_b was fully optimized using B3LYP/6-31+G(d, p) by the SCRF solvation model implemented in Jaguar. It has been documented that current continuum models may yield misleading results when solvent molecules are actively involved in the reaction mechanism,[18,49] e.g., through a water-assisted proton-transfer process in which one water molecule acts both as a proton acceptor and donor to facilitate the reaction as in D_TS_b. The free energy of D_TS_b calculated using aug-cc-PVTZ basis set with the SCRF method in Jaguar was ca. 16 kcal/mol, which is 8 kcal/mol lower than the corresponding gas-phase result. This energy difference was considerably larger than the other results based on Jaguar SCRF calculations. To investigate the validity of this result, we calculated the free energy of D_TS_b using 3 other approaches: (1) we calculated the single point energy at the B3LYP/6-311++G(2df, p) level using the PCM model implemented in Gaussian98 based on the solvated, optimized, structure of Jaguar; (2) we optimized the structure and calculated the energy of D_TS_b at the B3LYP/6-31+G(d, p) level using up to 4 explicit water molecules to mimic the aqueous environment; (3) we used the SCRF model in Jaguar to calculate the single point energy based on the structure obtained from 2. All the calculations gave very similar results for the energy barrier (ca. 22 kcal/mol) with deviation less than 2 kcal/mol. (b) Since $HOCH_3$ group moves away as the active water molecule comes close to phosphate in aqueous solution, these data is obtained as free energy difference of $(HOCH_3+D\_TS_d) - (H_2O+HPO_4CH_3^-)$.
(51) Allin C.; Gerwert, K. *Biochem.* **2001**, *40*, 3037.

charge distributions and orbital changes at different states. Our results show that there do exist zwitterion like analogues following dissociative transition states. However they exist in the form of $PO_3^-HOCH_3 \cdot H_2O$ (see Table S1) rather than a true zwitterion form $PO_3^{2-}H^+OCH_3 \cdot H_2O$ as Bianciotto et al. claimed. Further, as the active water molecule attacks the PO_3 group of the complex, the $HOCH_3$ group moves away, showing that the zwitterion like analogue is actually a meta-stable complex of PO_3^- and methanol.

The computational characterization of the hydrolysis mechanism of the tri-phosphate ester is more complicated due to the large negative charge. In gas phase, the activation energy of the dissociative hydrolysis pathway of the reaction of tri-phosphate and one water molecule is still much lower than the associative hydrolysis pathway. This agrees with the results of mono-phosphate mono-ester. However, the reaction barriers are very close in aqueous solution with difference less than 3.6 kcal/mol (see Table 4). In fact, without the assistance of the bridge water the dissociative process is higher in activation energy than the associative process by 3.4 kcal/mol. Because the energy difference between the associative and dissociative pathways is less than 4 kcal/mol, it is hard to conclude with absolute confidence which process is more favorable due to the uncertainties in the calculation of such large systems where environmental effects are so important. The calculation suggests that both processes are possible and competitive in aqueous solution with the dissociative pathway being slightly more favorable in this case. We caution that GTP hydrolysis mechanism in ras may be different, and more favorable process strongly depends on the protein environment.

When two water molecules, one acts as a nucleophile and the other mainly structural, were considered in the hydrolysis of tri-phosphate at least two transition states were found for the associative pathways. The first corresponds to proton transfer from the attacking water to $P_\gamma O_3$ and the second to P−O bond dissociation. The structural water did not significantly change the dissociative pathway, and the transition states of the reaction of tri-phosphate with two water molecules are very similar to the corresponding transition states of the reaction of tri-phosphate with one water molecule. The structural water appears to have small effects on the activation energy of either the associative or dissociative reaction pathways (see Table 3 and Table 4). In fact, inclusion of up to 4 water molecules in our calculations does not significantly change our results for the tri-phosphate (data not shown).

It is generally accepted that P−O bond cleavage in GTP hydrolysis follows a prior proton transfer from the catalytic water molecule to the general base, which most likely is GTP itself.[13] However, the idea of GTP itself acting as the general base has been challenged by some workers,[52] and whether GTP hydrolysis is a concerted or stepwise process is still not clear. In ref 13, Glennon et al. extensively analyzed the possibility of concerted vs stepwise process of GTP hydrolysis in Ras-GAP, and concluded that the reaction is a stepwise process, most likely involving an associative mechanism. As our results show, the reaction of $TME(H)^{3-} + H_2O$ is concerted, whereas the reaction of $TME(H)^{3-} + 2H_2O$ is a stepwise process, with the activation energy of the two reactions being very close. Because the difference is very small, it is difficult to conclude which pathway is more feasible in this case. To verify whether the hydrolysis of GTP itself is a concerted or stepwise process, further studies including the active residues is needed. Such studies are under way in our group.

As shown in Table 5, in the associative pathway charges shift from $P_\gamma O_3$ to $P_\beta O_3$ through the bridge oxygen as the nucleophilic water attacks $P_\gamma O_3$ resulting in P−O bond cleavage. In ref 7, the authors speculated that in the extreme case of dissociative process, there must be a loss of charge on the γ phosphoryl group being transferred, most likely to the β phosphate through the bridge oxygen to maintain conservation of charge. However, in our model, the P−O bond cleavage is initiated by the proton transfer from the γ phosphate to the bridge oxygen with no significant charge shift from the γ phosphoryl group to the β phosphate, based on an analysis of atomic charges derived from the electrostatic potential.

Because there is significant charge redistribution in the associative transition states compared to the reactant complex, the reaction barrier of the associative pathway is very sensitive to the environmental dielectric constant. High dielectric constant solvent, such as water, significantly reduced the energy barrier of the associative hydrolysis pathway reflecting the contribution of the environment to the charge redistribution. In contrast, no obvious charge redistribution occurred in the dissociative hydrolysis pathway in our model, causing the energy barrier of the dissociative hydrolysis pathway to be less sensitive to the dielectric reaction field. This suggests that the associative pathway may possibly be more susceptible to stabilization by the protein environment than the dissociative pathway, although more of the active site must be included to test this possibility. Figure 6 shows that in the gas phase, the energy barrier of the associative pathway is much higher than those of dissociative pathways a and b, whereas in aqueous solvent, the energy barrier of the associative pathway is lower than dissociative pathway a (without water molecule assisting proton transfer) but still higher than dissociative pathway b (with water molecule assisting proton transfer). The X-ray crystal structure of ras protein [121p] shows that, in the active site containing GTP, there is no space allowing a water molecule to participate in the proton transfer in the dissociative pathway as seen in dissociative pathway b. We therefore speculate that in the protein environment, the associative hydrolysis mechanism of GTP could be more favorable. However, the local protein environment, such as the divalent metal ion magnesium and other active site residues may influence the associative vs dissociative balance. Further calculations of GTP hydrolysis, including the active residues of ras and ras-GAP proteins, are being performed in our group.

Conclusions

Using a combination of DFT and dielectric continuum solvation methods, we have studied the possible hydrolysis pathways of mono-phosphate and tri-phosphate esters in gas phase and aqueous solution. For the mono-phosphate monoanion the dissociative process is more favorable than the associative process, especially when an additional water molecule plays an active role in the dissociative process. For the tri-phsosphate ester the energy barrier of the dissociative pathway is very close to that of the associative pathway, suggesting that both pathways are possible alternatives. In the associative pathway, charge

(52) Admiraal, S. J.; Herschlag, D. *J. Am. Chem. Soc.* **2000**, *122*, 2145−2148.

redistribution from the $P_\gamma O_3$ group to the $P_\beta O_3$ group through the bridge oxygen was significant as the nucleophilic water attacks the P_γ. This charge redistribution was not found in the dissociative process. High dielectric solvents, such as water, significantly reduce the reaction barrier of the associative pathway but have much less effect on the energy barrier of the dissociative pathway.

Acknowledgment. We thank the staff and administration of the Advanced Biomedical Computing Center and the National Cancer Institute for their support of this work. This project has been funded in whole or in part with federal funds from the National Cancer Institute, National Institutes of Health under Contract No. NO1-CO-12400. The content of this publication does not necessarily reflect the views or policies of the Department of Health and Human Services, nor does mention of trade names, commercial products, or organization imply endorsement by the U.S. Government.

Supporting Information Available: Structures (Figure S1) and charge distribution (Table S1) of the zwitterions analogue, relative energies (kcal/mol) of the stationary points for the reactions of $CH_3PO_4H^- + H_2O$ (Table S2), GTP-3-H + H_2O (Table S3), GTP-3-H + $2H_2O$ (Table S4) obtained from GAUSSIAN calculations using PCM model, and charge distribution on the stable states of reaction: $TME(H)3^- + 2H_2O$ obtained at HF/6-31+G(d,p) level (Table S5) (PDF). This material is available free of charge via the Internet at http://pubs.acs.org.

JA0279794